

RFN: A Random-Feature Based Newton Method for Empirical Risk Minimization in Reproducing Kernel Hilbert Spaces

Ting-Jui Chang and Shahin Shahrampour

Texas A&M University

E-mail: tingjui.chang@tamu.edu, shahin@tamu.edu

Abstract

In supervised learning using kernel methods, we encounter a large-scale finite-sum minimization over a reproducing kernel Hilbert space (RKHS). Often times large-scale finite-sum problems can be solved using efficient variants of Newton's method where the Hessian is approximated via sub-samples. In RKHS, however, the dependence of the penalty function to kernel makes standard sub-sampling approaches inapplicable, since the gram matrix is not readily available in a low-rank form. In this paper, we observe that for this class of problems, one can naturally use kernel approximation to speed up the Newton's method. Focusing on randomized features for kernel approximation, we provide a novel second-order algorithm that enjoys local superlinear convergence and global convergence in the high probability sense. The key to our analysis is showing that the approximated Hessian via random features preserves the spectrum of the original Hessian. We provide numerical experiments verifying the efficiency of our approach, compared to variants of sub-sampling methods.

1 Introduction

At the heart of many (supervised) machine learning problems, a learner must solve the following risk minimization

$$\min_{\mathbf{w} \in \mathbb{R}^d} \left\{ F(\mathbf{w}) \triangleq \sum_{i=1}^n \ell(y_i, f(\mathbf{x}_i; \mathbf{w})) + \lambda R(\mathbf{w}) \right\}, \quad (1)$$

where $\{(\mathbf{x}_i, y_i)\}_{i=1}^n$ are input-output data samples generated independently from an unknown distribution, ℓ is a task-dependent loss function, and R is a regularizer. Furthermore, f is a certain function class, parameterized by \mathbf{w} , on which the learner wants to minimize the risk. As an example, for linear models we simply have $f(\mathbf{x}; \mathbf{w}) = \mathbf{x}^\top \mathbf{w}$.

First-order optimization algorithms have been widely used to solve large-scale optimization problems of form (1) (e.g., see [1] for a recent survey). Relying solely on the gradient information, these methods converge to (local) optima. However, second-order algorithms employ the curvature information to properly re-scale the gradient, resulting in more appropriate directions and much faster convergence rates. As an example, in the unconstrained optimization, Newton’s method pre-multiplies the gradient by Hessian inverse at each iteration. It is quite well-known that under some technical assumptions, Newton’s method can achieve a locally super-linear convergence rate (see e.g., Theorem 1.2.5 in [2]). However, the cost of Hessian inversion is the major drawback of Newton’s method in practice.

To improve the (per iteration) time complexity, various approaches have been explored in the literature for approximately capturing the Hessian information. Popular methods in this direction include sub-sampling the Hessian matrix [3–5], sketching techniques [6], as well as quasi-Newton methods [7–10] and its stochastic variants [11–20].

Nevertheless, when the function class of f in (1) is a reproducing kernel Hilbert space (RKHS), due to the special structure of the problem, some of the aforementioned methods are not directly applicable and need some adjustments.

1.1 Risk Minimization in RKHS

In this paper, we restrict our attention to risk minimization in the case that the function f in (1) belongs to a RKHS. In particular, consider a symmetric positive-definite function $k(\cdot, \cdot)$ such that

$$\sum_{i,j=1}^n \alpha_i \alpha_j k(\mathbf{x}_i, \mathbf{x}_j) \geq 0,$$

for $\boldsymbol{\alpha} = [\alpha_1, \dots, \alpha_n]^\top \in \mathbb{R}^n$. Then, $k(\cdot, \cdot)$ is called a positive (semi-)definite kernel and can define a Hilbert space \mathcal{H} where $f(\mathbf{x}; \mathbf{w}) = \sum_{i=1}^n w_i k(\mathbf{x}, \mathbf{x}_i)$. This class of functions forms the basis of kernel methods that are powerful tools for data representation and are commonly used in machine learning. In

this scenario, the objective function takes the following form

$$F(\mathbf{w}) = \sum_{i=1}^n \ell\left(y_i, \sum_{j=1}^n w_j k(\mathbf{x}_i, \mathbf{x}_j)\right) + \frac{\lambda}{2} \|f\|_{\mathcal{H}}^2, \quad (2)$$

where the regularizer in (1) is the RKHS norm. Let us denote the kernel (gram) matrix as $[\mathbf{K}]_{ij} = k(\mathbf{x}_i, \mathbf{x}_j)$. The definition of inner product in RKHS immediately implies that $\|f\|_{\mathcal{H}}^2 = \mathbf{w}^\top \mathbf{K} \mathbf{w}$ (see e.g., page 62 of [21]). Then, assuming that ℓ is twice-differentiable, the Hessian of the objective function in (2) can be calculated as follows

$$\mathbf{H}(\mathbf{w}) \triangleq \nabla^2 F(\mathbf{w}) = \mathbf{K} \mathbf{D}(\mathbf{w}) \mathbf{K} + \lambda \mathbf{K}, \quad (3)$$

where $\mathbf{D}(\mathbf{w}) \in \mathbb{R}^{n \times n}$ is a diagonal matrix defined as

$$[\mathbf{D}(\mathbf{w})]_{ii} = \ell''\left(y_i, \sum_{j=1}^n w_j k(\mathbf{x}_i, \mathbf{x}_j)\right). \quad (4)$$

Observe that in (3), the diagonal structure of $\mathbf{D}(\mathbf{w})$ and the symmetry of \mathbf{K} together imply that $\mathbf{K} \mathbf{D}(\mathbf{w}) \mathbf{K}$ can be trivially represented as a sum of rank-one matrices. However, \mathbf{K} , which appears as a result of the regularization term, may be dense and not readily available in a low-rank form. In other words, decomposing \mathbf{K} to a low-rank matrix also requires effort, so we cannot directly apply subsampling Newton techniques, such as those in [5, 3, 4] to optimize the objective function (2). This naturally raises the following question, which we pursue in this paper:

Problem 1. *Given the explicit connection of the Hessian (3) to the gram matrix \mathbf{K} , can we use kernel approximation techniques to speed up the Newton method?*

1.2 Our Contributions

In this paper, we answer to Problem 1 in the affirmative by providing the following contributions:

- We apply the idea of randomized features for kernel approximation [22] to approximate the Hessian (3). Our algorithm is thus dubbed Random-Feature based Newton (RFN). The detailed derivation of RFN is explained in Section 2.

- The key to our technical analysis is Lemma 2, which shows that when enough random features are sampled, the approximate Hessian is close to $\mathbf{H}(\mathbf{w})$ in the spectral norm sense. Our analysis relies on matrix concentration inequalities rather than refining standard guarantees in the kernel approximation literature.
- We prove that RFN enjoys local superlinear convergence and global convergence in the high probability sense (Section 3).
- Our numerical experiments on real-world datasets (Section 4) provide a performance comparison among RFN, classical Newton, L-BFGS, and a variation of sub-sampled Newton methods (as they are not directly applicable to (2)). We illustrate that RFN achieves a superior loss vs. run-time rate against its competitors. We also investigate the sensitivity of RFN with respect to a number of hyper-parameters.

We have included the omitted proofs in the Appendix (Section 6).

1.3 Related Literature

Inspired by the success of stochastic first-order algorithms for large-scale data analytics, the stochastic forms of second-order optimization have received more attention in the recent literature. In this section, we will discuss several stochastic second-order methods and we split them into two categories: quasi-Newton methods and second-order Hessian-based methods.

– **Quasi-Newton Methods:** Instead of doing the expensive computation of the Newton step (which involves Hessian inversion), quasi-Newton methods approximate the Hessian by using the information obtained from gradient evaluations. BFGS algorithm [7–10] is a seminal work of this type. Recent works [11–20] in this area have focused on stochastic quasi-Newton methods to obtain curvature information in a computationally inexpensive manner. Mokhtari and Ribeiro [12] propose a stochastic regularized version of BFGS algorithm to avoid the problem of singular curvature estimates and provide convergence

of the sequence to optimal arguments in expectation. Byrd et al. [13] apply sub-sampled Hessian-vector products to stabilize the curvature estimation based on a stochastic limited memory BFGS (L-BFGS) algorithm. An interesting advancement in this line of work is provided by Moritz et al. [14] who propose an algorithm based on L-BFGS by incorporating ideas from stochastic variance-reduced gradient (SVRG) to achieve linear convergence to the optimum. Gower et al. [19] employ the idea of SVRG to propose a stochastic block BFGS algorithm using sketching techniques and show practical speed-ups for common machine learning problems. Based on the algorithm structure of [14], Zhao et al. [20] propose a coordinate transformation framework to analyze stochastic L-BFGS type algorithms and present improved convergence rates and computational complexities.

– **Second-Order Hessian based Methods:** The appealing feature of Newton’s method is its fast convergence rate. However, there are two main issues for the implementation of the classical Newton method: the cost of Hessian construction, and the cost of Hessian inversion. For example, in application to the family of generalized linear models (GLMs) involving an $n \times d$ data matrix, the computation of the full Hessian costs $O(nd^2)$ and the matrix inversion takes $O(d^3)$ time. This high cost, especially for large-scale applications, has motivated researchers to apply randomization techniques, and thus sub-sampled Newton methods have gained a good deal of attention recently.

In [23, 24], the authors establish the convergence of the modified Newton’s method with sub-sampled Hessian. Under a similar setting to [23, 24], Wang et al. [25] provide modifications in order to get better estimated Hessian and time cost performance. Within the context of deep neural networks, Martens [26] proposes a sub-sampled Gauss-Newton method for the training and studies the choice of the regularization parameter.

Erdogdu and Montanari [27] propose a Newton-like method, where the Hessian is approximated by sub-sampling the true Hessian and computing its truncated eigenvalue decomposition. Their work establishes non-asymptotic local convergence rates for the uniform sub-sampling of the Hessian. Pilanci

and Wainwright [6] propose another Hessian approximation method, called Newton sketching, which approximates the true Hessian through random projection matrices. This method is applicable for the case where the square root of the full Hessian is available and the best complexity results are achieved when the randomized Hadamard transform is used.

Authors of [3, 4] analyze the global and local convergence rates for sub-sampled Newton methods with different sampling rates for gradient and Hessian approximations. Bollapragada et al. [3] show their convergence results in expectation whereas [4] provides high probability guarantees by applying matrix concentration inequalities [28, 29]. The work of [4] further relaxes a common assumption in the literature: though the objective function is assumed to be strongly convex, the individual functions are only weakly convex. Along this line of works, Xu et al. [5] build the approximated Hessian by applying non-uniform sampling based on the data matrix to get better dependence on problem specific quantities.

Agarwal et al. [30] propose a method to compute an unbiased estimator of the inverse Hessian based on the power expansion of the Hessian inverse. The method achieves a time complexity scaling linearly with the size of variables. This is followed by an improved and simplified convergence analysis in [31].

The main distinction of our work with prior art is that we consider minimization in RKHS, where there are explicit connections between the Hessian and the gram matrix. We leverage this fact to approximate the Hessian, and we provide theoretical guarantees for our method.

2 Random-Feature Based Newton Method

2.1 Notation

We denote by $\text{Tr}[\cdot]$ the trace operator, by $\langle \cdot, \cdot \rangle$ the standard inner product, by $\|\cdot\|$ the spectral (respectively, Euclidean) norm of a matrix (respectively, vector), by $O(\cdot)$ (respectively, $\Omega(\cdot)$) the Big O (respectively, Big Omega) notation in complexity theory, and by $\mathbb{E}[\cdot]$ the expectation operator. Boldface lowercase variables (e.g., \mathbf{a}) are used for vectors, and boldface uppercase variables (e.g., \mathbf{A}) are used for matrices. $[\mathbf{A}]_{ij}$ denotes the ij -th entry of matrix \mathbf{A} . $\lambda_{\min}(\mathbf{A})$ (respectively, $\lambda_{\max}(\mathbf{A})$) denotes the smallest (re-

spectively, largest) eigenvalue of matrix \mathbf{A} . The symbol “ \preceq ” is used for matrix inequality and $\mathbf{A} \preceq \mathbf{B}$ implies that the matrix $(\mathbf{B} - \mathbf{A})$ is positive semi-definite. $|\mathcal{I}|$ represents the cardinality of the set \mathcal{I} . The vectors are all in column form.

2.2 Background on Random Features for Kernel Approximation

As discussed in the Introduction, the Hessian of the objective function in (2) can be written as $\mathbf{H}(\mathbf{w}) = \mathbf{K}\mathbf{D}(\mathbf{w})\mathbf{K} + \lambda\mathbf{K}$, where $[\mathbf{K}]_{ij} = k(\mathbf{x}_i, \mathbf{x}_j)$ is the gram matrix. The Hessian is a square matrix of size n and a plain inversion of that in Newton’s method introduces a prohibitive cost of $O(n^3)$. With n being the number of data points, this cost is specifically expensive for big data problems.

To find a low-rank representation of Hessian, the key is to approximate the gram matrix $\mathbf{K} \in \mathbb{R}^{n \times n}$, which in general is dense. An elegant method for kernel approximation, called random Fourier features, is introduced by Rahimi and Recht [22]. Let $\tau(\boldsymbol{\omega})$ be a probability density with support $\Omega \subseteq \mathbb{R}^d$. Consider any kernel function with the following integral form

$$k(\mathbf{x}, \mathbf{x}') = \int_{\Omega} \phi(\mathbf{x}, \boldsymbol{\omega})\phi(\mathbf{x}', \boldsymbol{\omega})\tau(\boldsymbol{\omega})d\boldsymbol{\omega}, \quad (5)$$

where $\phi(\mathbf{x}, \boldsymbol{\omega}) : \mathbb{R}^d \rightarrow \mathbb{R}$ is a feature map. We can immediately see from (5) that the kernel function can be approximated via Monte-Carlo sampling as

$$k(\mathbf{x}, \mathbf{x}') \approx \frac{1}{m} \sum_{s=1}^m \phi(\mathbf{x}, \boldsymbol{\omega}_s)\phi(\mathbf{x}', \boldsymbol{\omega}_s), \quad (6)$$

where $\{\boldsymbol{\omega}_s\}_{s=1}^m$ are independent samples from the density $\tau(\boldsymbol{\omega})$ and are called *random features*. There exist many kernels taking the form (5), including shift-invariant kernels [22] and dot product (e.g., polynomial) kernels [32] (see Table 1 in [33] for an exhaustive list). Gaussian kernel, for example, can be approximated using $\phi(\mathbf{x}, \boldsymbol{\omega}) = \sqrt{2} \cos(\boldsymbol{\omega}^\top \mathbf{x} + b)$ where $\boldsymbol{\omega}$ follows a Gaussian distribution and b has a uniform distribution on $[0, 2\pi]$. It is common to assume that the feature map is uniformly bounded (as evident in the case of cosine).

We now define

$$\mathbf{z}(\boldsymbol{\omega}) \triangleq [\phi(\mathbf{x}_1, \boldsymbol{\omega}), \dots, \phi(\mathbf{x}_n, \boldsymbol{\omega})]^\top. \quad (7)$$

Then, the gram matrix \mathbf{K} can be approximated with $\mathbf{Z}\mathbf{Z}^\top$ where $\mathbf{Z} \in \mathbb{R}^{n \times m}$ is the following matrix

$$\mathbf{Z} \triangleq \frac{1}{\sqrt{m}}[\mathbf{z}(\boldsymbol{\omega}_1), \dots, \mathbf{z}(\boldsymbol{\omega}_m)]. \quad (8)$$

When $m < n$ in above, the approximation of \mathbf{K} is low-rank, saving computational cost when used to find the Newton direction. Avron et al. [34] prove the following ϵ -spectral approximation guarantee for $\mathbf{K} \approx \mathbf{Z}\mathbf{Z}^\top$:

Theorem 1. [34] *Let $\epsilon \in (0, 1/2]$ and $\delta \in (0, 1)$ be fixed constants. Assume that $\|\mathbf{K}\|_2 \geq \gamma$. If we use $m \geq \frac{8}{3}\epsilon^{-2}\frac{n}{\gamma} \ln(16S_\gamma(\mathbf{K})/\delta)$ random Fourier features (sampled from $\tau(\boldsymbol{\omega})$), the following identity holds*

$$(1 - \epsilon)(\mathbf{K} + \gamma\mathbf{I}) \preceq \mathbf{Z}\mathbf{Z}^\top + \gamma\mathbf{I} \preceq (1 + \epsilon)(\mathbf{K} + \gamma\mathbf{I}), \quad (9)$$

with probability at least $1 - \delta$, where $S_\gamma(\mathbf{K}) \triangleq \text{Tr}[\mathbf{K}(\mathbf{K} + \gamma\mathbf{I})^{-1}]$.

In view of (9), $\mathbf{Z}\mathbf{Z}^\top + \gamma\mathbf{I}$ is dubbed an ϵ -spectral approximation of $\mathbf{K} + \gamma\mathbf{I}$. Theorem 1 characterizes the number of random features required to achieve an ϵ -spectral approximation of the kernel matrix given a specific γ . Nevertheless, if we apply this result to approximate the Hessian (3) in a plug-and-play fashion, the number of required features would be $m = \Omega(\epsilon^{-2})$. In Lemma 2, we establish a novel bound specifically for approximation of the Hessian $\mathbf{H}(\cdot)$, where the dependence has the potential to be improved to $m = \Omega(\epsilon^{-1})$.

2.3 Main Algorithm: Random-Featured Based Newton (RFN)

We now leverage the random feature approximation, introduced in the previous section, for Hessian approximation. Following (3) and using the approximation $\mathbf{K} \approx \mathbf{Z}\mathbf{Z}^\top$, where \mathbf{Z} is given in (8), we derive

$$\widehat{\mathbf{H}}(\mathbf{w}) = \mathbf{Z}\mathbf{Z}^\top \mathbf{D}(\mathbf{w})\mathbf{Z}\mathbf{Z}^\top + \lambda\mathbf{Z}\mathbf{Z}^\top. \quad (10)$$

Algorithm 1 Random-Feature Based Newton (RFN)

- 1: **Input:** Initial point \mathbf{w}_0 , # of iterations t_0 , # of random features m , density function of random features $\tau(\boldsymbol{\omega})$, hyper-parameters for backtracking line search, regularization parameters $\lambda, \mu > 0$.
 - 2: **Output:** \mathbf{w}_{t_0}
 - 3: **for** $t = 0$ **to** $t_0 - 1$ **do**
 - 4: Sample m independent random features from τ and construct the feature matrix \mathbf{Z} as in (8).
 - 5: Compute $\mathbf{g}(\mathbf{w}_t) = \nabla F(\mathbf{w}_t)$, the gradient of the objective (2).
 - 6: Compute $\widehat{\mathbf{H}}_\mu^{-1}(\mathbf{w}_t)$ as given in (12).
 - 7: Update $\mathbf{w}_{t+1} = \mathbf{w}_t - \alpha_t \widehat{\mathbf{H}}_\mu^{-1}(\mathbf{w}_t) \mathbf{g}(\mathbf{w}_t)$, where α_t is selected via backtracking line search.
 - 8: **end for**
-

It is immediate that when $m < n$, the above approximated Hessian is singular, so in order to make $\widehat{\mathbf{H}}(\mathbf{w})$ invertible, a regularization term $\mu \mathbf{I}$ (for some $\mu > 0$) is added to the above, and the new approximate can be written as,

$$\widehat{\mathbf{H}}_\mu(\mathbf{w}) \triangleq \mathbf{Z} \left[\mathbf{Z}^\top \mathbf{D}(\mathbf{w}) \mathbf{Z} + \lambda \mathbf{I} \right] \mathbf{Z}^\top + \mu \mathbf{I}. \quad (11)$$

Let $\mathbf{C}(\mathbf{w}) \triangleq \mathbf{Z}^\top \mathbf{D}(\mathbf{w}) \mathbf{Z} + \lambda \mathbf{I}$. By matrix inversion lemma, $\widehat{\mathbf{H}}_\mu^{-1}(\mathbf{w})$ can be written as

$$\widehat{\mathbf{H}}_\mu^{-1}(\mathbf{w}) = \frac{1}{\mu} \left[\mathbf{I} - \mathbf{Z} \left(\mu \mathbf{C}^{-1}(\mathbf{w}) + \mathbf{Z}^\top \mathbf{Z} \right)^{-1} \mathbf{Z}^\top \right], \quad (12)$$

which can reduce the time complexity of computing $\widehat{\mathbf{H}}_\mu^{-1}(\mathbf{w}) \nabla F(\mathbf{w})$ from $O(n^3)$ to $O(m^2 n + m^3)$. Then, we can use $\widehat{\mathbf{H}}_\mu^{-1}(\mathbf{w})$ to perform a computationally efficient Newton update, as described in Algorithm 1.

2.4 Adjustment of Sub-sampled Newton Methods

We now revisit sub-sampled Newton methods to elaborate on the differences between RFN and these methods. Sub-sampled Newton algorithms often end up working with Hessians of the form

$$\mathbf{H}(\mathbf{w}) = \frac{1}{n} \sum_{i=1}^n \mathbf{a}_i(\mathbf{w}) \mathbf{a}_i^\top(\mathbf{w}) + \mathbf{Q}(\mathbf{w}),$$

where $\mathbf{a}_i(\mathbf{w})$ is a vector and $\mathbf{Q}(\mathbf{w})$ is a data-independent matrix (see e.g., [5]). Given this structure, if we randomly select a subset \mathcal{I} of data points, the Hessian can be easily approximated via

$$\widehat{\mathbf{H}}(\mathbf{w}) = \frac{1}{|\mathcal{I}|} \sum_{i \in \mathcal{I}} \mathbf{a}_i(\mathbf{w}) \mathbf{a}_i^\top(\mathbf{w}) + \mathbf{Q}(\mathbf{w}).$$

This would reduce the time cost of Hessian construction by a factor of $|\mathcal{I}|/n$. Furthermore, since the approximated Hessian still consists of sum of rank-one matrices (in the data-related part), one can apply conjugate gradient (CG) method when computing the newton step to further speed up the process [5, 4, 3].

However, it turns out that the Hessian of the objective function (2), i.e., $\mathbf{K}\mathbf{D}(\mathbf{w})\mathbf{K} + \lambda\mathbf{K}$, cannot be directly handled by sub-sampling, since the regularizer in this case is indeed *data-dependent* and writing it as a sum of rank-one matrices requires a low-rank decomposition. In this case, sub-sampled Newton techniques can be adjusted using the Nyström method for column sampling (see e.g., [35] for a review on Nyström). Let $\mathcal{V} = \{1, \dots, n\}$ and \mathcal{I} denote a (random) subset of \mathcal{V} . Furthermore, denote by $\mathbf{K}(\mathcal{A}, \mathcal{B})$ the sub-matrix of \mathbf{K} with rows in $\mathcal{A} \subseteq \mathcal{V}$ and columns in $\mathcal{B} \subseteq \mathcal{V}$. Then, the gram matrix \mathbf{K} can be approximated as

$$\mathbf{K} \approx \mathbf{K}(\mathcal{V}, \mathcal{I})\mathbf{K}(\mathcal{I}, \mathcal{I})^\dagger\mathbf{K}(\mathcal{I}, \mathcal{V}), \quad (13)$$

where \mathbf{M}^\dagger denotes the pseudo-inverse of \mathbf{M} . This decomposition introduces $O(n|\mathcal{I}|^2)$ time cost but circumvents the need for matrix inversion (by applying CG method). Notice that the first term of the Hessian can be trivially sub-sampled since

$$\mathbf{K}\mathbf{D}(\mathbf{w})\mathbf{K} = \sum_{i=1}^n [\mathbf{D}(\mathbf{w})]_{ii} \mathbf{K}(\mathcal{V}, i)\mathbf{K}(i, \mathcal{V}). \quad (14)$$

In the similar spirit as [5, 3, 4], we call this algorithm SSNCG, as it is a sub-sampled Newton method, where CG is used to find the Newton step.

Remark 1. *Since the focus of this work is on random features, we only compare RFN to the case that \mathcal{I} is chosen uniformly at random, i.e., the method would be a variant of uniform sub-sampled Newton [4]. Nonuniform sampling methods give better approximations of the kernel at the cost of modifying the uniform sampling distribution. We refer the reader to Table 1 in [35] for various guarantees on the approximation quality via different sampling schemes.*

2.5 Comparison of Time Complexity

We present the time complexity of finding the Newton step for four methods: Newton method, sub-sampled Newton method solved with CG exactly, sub-sampled Newton method solved with CG inexactly up to ε residual error, and random-feature based Newton method. The number of random features used by RFN is denoted by m . The size of the sub-sampled data points is $|\mathcal{I}|$, as discussed in Section 2.4. κ_{SSN} represents the upper bound of the condition number of the Hessian generated from sub-sampled data. Note that for each method, the reported complexity excludes the cost of obtaining the gradient, because that cost is the same for all methods.

Table 1: Time complexity per iteration.

Method	Complexity per iteration
Newton	$O(n^3)$
SSNCG (exact)	$O(\mathcal{I} n^2)$
SSNCG (inexact)	$O(\mathcal{I} ^2n + \mathcal{I} n\sqrt{\kappa_{SSN}} \log \varepsilon^{-1})$
RFN	$O(m^2n + m^3)$

3 Theoretical Results

In this section, we will study the convergence properties of our proposed method. In order to establish our results, we need to prove that the approximated Hessian mimics the original Hessian, which is shown in Lemma 2. Then, we can show the global and local convergence of RFN in Sections 3.2 and 3.3, respectively.

3.1 Preliminaries

Throughout the paper, we adhere to the following assumptions:

Assumption 1. (*Bounded Eigenvalues of Hessians*) *The objective function F is twice-differentiable, γ -strongly convex, and L -smooth. The smallest and largest eigenvalues of the Hessian are bounded as follows*

$$\gamma \mathbf{I} \preceq \mathbf{H}(\mathbf{w}) \triangleq \nabla^2 F(\mathbf{w}) \preceq L \mathbf{I}, \quad \forall \mathbf{w} \in \mathbb{R}^n, \quad (15)$$

and also $\mathbf{D}(\mathbf{w})$ satisfies

$$\|\mathbf{D}(\mathbf{w})\| \leq \lambda_1 < \infty, \quad \forall \mathbf{w} \in \mathbb{R}^n. \quad (16)$$

Condition (16) is satisfied for common loss functions (e.g. quadratic loss and logistic loss). Furthermore, if we solve the risk minimization (2) with a positive definite kernel, the gram matrix \mathbf{K} would be positive definite, and therefore, Assumption 1 is satisfied. We also define the condition number κ of the Hessian matrix as follows:

$$\kappa \triangleq \frac{L}{\gamma}. \quad (17)$$

Assumption 2. (*Lipschitz Continuity of Hessian*) *The Hessian of the objective function F is Lipschitz continuous, i.e., there exists a constant $M > 0$, such that*

$$\|\mathbf{H}(\mathbf{w}_1) - \mathbf{H}(\mathbf{w}_2)\| \leq M \|\mathbf{w}_1 - \mathbf{w}_2\|, \quad \forall \mathbf{w}_1, \mathbf{w}_2 \in \mathbb{R}^n. \quad (18)$$

Assumption 2 is also commonly used in the literature to establish superlinear convergence of sub-sampled Newton methods (see e.g., [3, 4]). Indeed, the assumption is used for superlinear convergence of the original Newton method as well (see e.g., Theorem 1.2.5 in [2]).

We are now ready to show that the approximated Hessian is close enough to the original Hessian when large enough random features are sampled.

Lemma 2. (*The spectrum preserving inequality*) *Suppose (16) holds. Given any $0 < \epsilon \leq \frac{3}{2} \|\mathbf{K}\| \min\{\text{Tr}(\mathbf{K})\lambda_1, \lambda\}$ and $0 < \delta < 1$, if*

$$m = \Omega \left(\frac{n^2}{\epsilon} \max \left\{ \frac{\lambda^2}{\epsilon} \log \frac{n}{\delta}, \lambda_1 \sqrt{\log \frac{n}{\delta}} \right\} \right),$$

then, we have that

$$\Pr \left(\left\| \widehat{\mathbf{H}}(\mathbf{w}) - \mathbf{H}(\mathbf{w}) \right\| \leq 4\epsilon \right) \geq 1 - \delta.$$

Corollary 3. *Under assumptions of Lemma 2, with probability at least $1 - \delta$, we have*

$$[(1 - \Psi)\gamma + \mu] \cdot \mathbf{I} \preceq \widehat{\mathbf{H}}_\mu(\mathbf{w}) \preceq [(1 + \Psi)L + \mu] \cdot \mathbf{I}, \quad (19)$$

where $\Psi \triangleq 4\epsilon/\gamma$, and μ is chosen such that $4\epsilon - \gamma < \mu$.

Proof. From Lemma 2, we have $\left\| \widehat{\mathbf{H}}(\mathbf{w}) - \mathbf{H}(\mathbf{w}) \right\| \leq \Psi\gamma$, which implies the following relationship

$$\begin{aligned} \mathbf{H}(\mathbf{w}) - \Psi\gamma \cdot \mathbf{I} &\preceq \widehat{\mathbf{H}}(\mathbf{w}) \preceq \mathbf{H}(\mathbf{w}) + \Psi\gamma \cdot \mathbf{I} \\ \implies (1 - \Psi)\mathbf{H}(\mathbf{w}) &\preceq \widehat{\mathbf{H}}(\mathbf{w}) \preceq (1 + \Psi)\mathbf{H}(\mathbf{w}) \\ \implies (1 - \Psi)\mathbf{H}(\mathbf{w}) + \mu \cdot \mathbf{I} &\preceq \widehat{\mathbf{H}}_\mu(\mathbf{w}) \preceq (1 + \Psi)\mathbf{H}(\mathbf{w}) + \mu \cdot \mathbf{I} \end{aligned} \quad (20)$$

By applying (15) to (20), (19) is proved. \square

Notice that proving Lemma 2 with standard results in the literature of kernel approximation yields weaker guarantees. In particular, using ϵ -spectral approximation results (e.g., Theorem 1) or spectral norm errors for kernel approximation (e.g., Eq. (6.5.7) in [29]) give rise to $m = \Omega(\epsilon^{-2})$. However, Lemma 2 shows that the number of required features depends on the interplay of several parameters. In particular, when the regularization parameter λ is small enough, $m = \Omega(\epsilon^{-1})$ since we are mainly concerned with approximating $\mathbf{KD}(\mathbf{w})\mathbf{K}$ in (3). In particular, (disregarding the log-factors) when for a given $\epsilon > 0$, we choose $\lambda^2 \leq \lambda_1\epsilon$, we have that $m = \Omega(\epsilon^{-1})$, which is a blessing obtained by regularization. On the other hand, $m = \Omega(n^2)$ suggests worse dependence on n compared to Theorem 1, where $m = \Omega(n)$. However, this is due to the fact that we look at an error bound that depends on ϵ , which is rather different from (9), where the spectral inequality depends on $\epsilon\mathbf{K}$.

Remark 2. *For the rest of the paper, we assume that ϵ and μ satisfy the constraints in Lemma 2 and Corollary 3.*

3.2 Global Linear Convergence

In this section, we will show the global convergence of our method with the spectral approximation inequality derived in Lemma 2. Recall that the update of the iterate is written as

$$\mathbf{w}_{t+1} = \mathbf{w}_t + \alpha_t \mathbf{p}_t, \quad (21)$$

where $\mathbf{p}_t \triangleq -[\widehat{\mathbf{H}}_\mu(\mathbf{w}_t)]^{-1} \nabla F(\mathbf{w}_t)$ and α_t is selected by Armijo-type line search such that

$$F(\mathbf{w}_t + \alpha_t \mathbf{p}_t) \leq F(\mathbf{w}_t) + \alpha_t \beta \mathbf{p}_t^\top \nabla F(\mathbf{w}_t), \quad (22)$$

for some $\beta \in (0, 1)$. In what follows, we denote the minimizer of $F(\mathbf{w})$ by \mathbf{w}^* .

Theorem 4. (*Global convergence*) *Let Assumption 1 hold. If we update $\mathbf{w}_t \in \mathbb{R}^n$ using RFN algorithm, where $\widehat{\mathbf{H}}_\mu(\mathbf{w}_t)$ is constructed by sampling*

$$m = \Omega \left(\frac{n^2}{\epsilon} \max \left\{ \frac{\lambda^2}{\epsilon} \log \frac{n}{\delta}, \lambda_1 \sqrt{\log \frac{n}{\delta}} \right\} \right),$$

random features, we have

$$F(\mathbf{w}_{t+1}) - F(\mathbf{w}^*) \leq (1 - \rho_t)(F(\mathbf{w}_t) - F(\mathbf{w}^*)),$$

with probability at least $1 - \delta$, where

$$\rho_t \triangleq \frac{2\alpha_t\beta\gamma}{(1 + \Psi)L + \mu}.$$

Moreover, the step size $\alpha_t \leq 2(1 - \beta)[(1 - \Psi)\gamma + \mu]/L$ is sufficient to pass the line search.

Theorem 4 draws a connection between the precision of approximated Hessian and the convergence speed. If the precision parameter Ψ is set to a small number (high precision), the step size α_t is upper bounded by a larger number, which implies a more aggressive update. Also, the parameter ρ_t tends to be larger (i.e., faster convergence) if the approximated Hessian is closer to the true one.

3.3 Local Superlinear Convergence

The classical Newton's method is appealing particularly for its local convergence property, resulting in quadratic rates for strongly convex and smooth problems. In this section, we are going to discuss the local convergence behavior of our method. For the local case, we consider using a unit step size, i.e., $\alpha_t = 1$. In the following lemma, we provide an error recursion for the update \mathbf{w}_t using Lemma 2.

Lemma 5. (*Error recursion*) *Let Assumptions 1-2 hold. If we update $\mathbf{w}_t \in \mathbb{R}^n$ using RFN algorithm (with $\alpha_t = 1$), where $\widehat{\mathbf{H}}_\mu(\mathbf{w}_t)$ is constructed by sampling*

$$m = \Omega \left(\frac{n^2}{\epsilon} \max \left\{ \frac{\lambda^2}{\epsilon} \log \frac{n}{\delta}, \lambda_1 \sqrt{\log \frac{n}{\delta}} \right\} \right),$$

random features, we have

$$\|\mathbf{w}_{t+1} - \mathbf{w}^*\| \leq \nu \|\mathbf{w}_t - \mathbf{w}^*\| + \eta \|\mathbf{w}_t - \mathbf{w}^*\|^2, \quad (23)$$

with probability at least $1 - \delta$, where

$$\nu \triangleq \frac{\Psi\gamma + \mu}{(1 - \Psi)\gamma + \mu} \quad \text{and} \quad \eta \triangleq \frac{M}{2[(1 - \Psi)\gamma + \mu]}. \quad (24)$$

The above lemma helps with establishing the convergence given a certain range of ϵ , as discussed in the following theorem.

Theorem 6. (*Local linear convergence*) *Let Assumptions 1-2 hold. Suppose ϵ is chosen such that $0 < \nu < 1$ and ρ is selected as*

$$\nu < \rho < 1.$$

Assume the initial point \mathbf{w}_0 satisfies

$$\|\mathbf{w}_0 - \mathbf{w}^*\| \leq \frac{\rho - \nu}{\eta}, \quad (25)$$

where η is defined in Lemma 5. If we update $\mathbf{w}_t \in \mathbb{R}^n$ using RFN algorithm (with $\alpha_t = 1$), where $\widehat{\mathbf{H}}_\mu(\mathbf{w}_t)$ is constructed by sampling

$$m = \Omega \left(\frac{n^2}{\epsilon} \max \left\{ \frac{\lambda^2}{\epsilon} \log \frac{n}{\delta}, \lambda_1 \sqrt{\log \frac{n}{\delta}} \right\} \right),$$

random features, we have the following linear convergence

$$\|\mathbf{w}_t - \mathbf{w}^*\| \leq \rho \|\mathbf{w}_{t-1} - \mathbf{w}^*\|, \quad t = 1, \dots, t_0 \quad (26)$$

with probability $(1 - t_0\delta)$.

If the precision of the Hessian approximation increases through iterations, it is expected that the algorithm can converge faster than the linear rate. In the next theorem, we show that if the Hessian approximation error decreases geometrically, RFN converges superlinearly.

Theorem 7. (*Local superlinear convergence*) Let the assumptions of Theorem 6 hold. Also, for each iteration t , $t = 0, 1, \dots, t_0$ define the quantities ϵ_t , ν_t and η_t as follows

$$\epsilon_t = \rho^t \epsilon, \quad \nu_t \triangleq \frac{6\epsilon_t}{\gamma - 2\epsilon_t} \quad \text{and} \quad \eta_t \triangleq \frac{M}{2(\gamma - 2\epsilon_t)},$$

where ν_t and η_t are defined by setting $\mu_t = 2\epsilon_t$ and substituting μ_t and ϵ_t into (24). Assume that \mathbf{w}_0 satisfies (25) with ρ , ν_0 and η_0 and update $\mathbf{w}_t \in \mathbb{R}^n$ using RFN algorithm (with $\alpha_t = 1$). Then, we have the superlinear convergence

$$\|\mathbf{w}_t - \mathbf{w}^*\| \leq \rho^t \|\mathbf{w}_{t-1} - \mathbf{w}^*\|, \quad t = 1, \dots, t_0, \quad (27)$$

with probability $(1 - t_0\delta)$.

Proof. The proof follows a similar argument to that of Theorem 7 in [4]. Based on Lemma 5, for each iteration t , sampling m random features such that the Hessian approximation error is at most ϵ_t , we have

$$\|\mathbf{w}_{t+1} - \mathbf{w}^*\| \leq \nu_t \|\mathbf{w}_t - \mathbf{w}^*\| + \eta_t \|\mathbf{w}_t - \mathbf{w}^*\|^2.$$

Note that, by $\epsilon_t = \rho^t \epsilon$, it follows that

$$\nu_t \leq \rho^t \nu_0$$

$$\eta_t \leq \eta_{t-1}.$$

Define $\Delta_t \triangleq \mathbf{w}_t - \mathbf{w}^*$. For $t = 0$, by assumption on ρ , ν_0 , and η_0 (Theorem 6), we have

$$\begin{aligned} \|\Delta_1\| &\leq \nu_0 \|\Delta_0\| + \eta_0 \|\Delta_0\|^2 \\ &\leq \rho \|\Delta_0\|. \end{aligned}$$

Assume (27) holds up to iteration t . For $t + 1$, we get

$$\begin{aligned} \|\Delta_{t+1}\| &\leq \nu_t \|\Delta_t\| + \eta_t \|\Delta_t\|^2 \\ &\leq \rho^t \nu \|\Delta_t\| + \eta_t \|\Delta_t\|^2 \\ &\leq \rho^t \nu \|\Delta_t\| + \eta_0 \|\Delta_t\|^2. \end{aligned}$$

By induction hypothesis, we have $\|\Delta_{t-1}\| \leq \|\Delta_0\|$, and

$$\|\Delta_t\| \leq \rho^t \|\Delta_{t-1}\| \leq \rho^t \left(\frac{\rho - \nu_0}{\eta_0} \right).$$

Therefore, it follows that $\|\Delta_{t+1}\| \leq \rho^{t+1} \|\Delta_t\|$. □

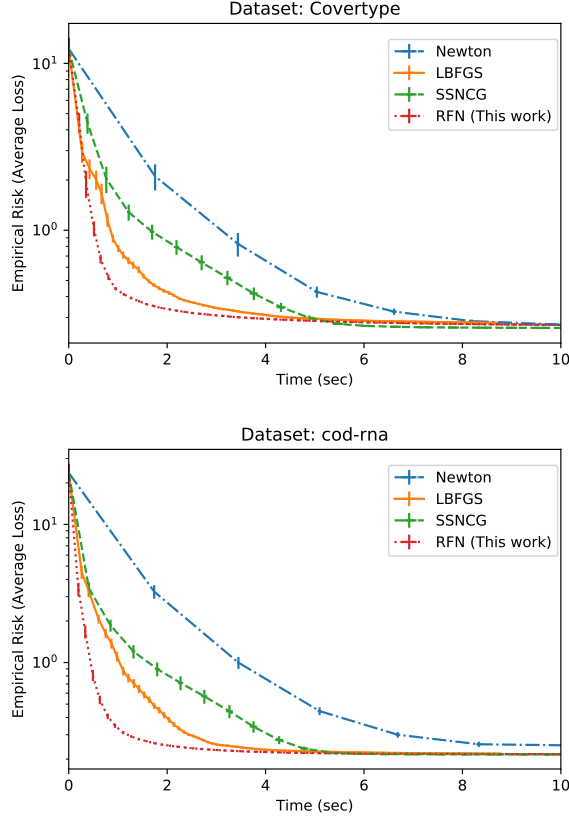


Figure 1: The plot of empirical risk (training error) vs. time cost shows that RFN enjoys a faster decay rate compared to other methods.

4 Numerical Experiments

We now provide numerical experiments to illustrate the performance of the random-feature based Newton method. We consider regularized kernel logistic regression

$$F(\mathbf{w}) = \frac{1}{n} \sum_{i=1}^n \log(1 + \exp(-y_i \sum_{j=1}^n k(\mathbf{x}_i, \mathbf{x}_j) w_j)) + \lambda \|\mathbf{w}\|_{\mathbf{K}}^2, \quad (28)$$

where $k(\mathbf{x}, \mathbf{x}') = e^{-\frac{\sigma^2 \|\mathbf{x} - \mathbf{x}'\|^2}{2}}$ is chosen to be a Gaussian kernel, and $\|\mathbf{w}\|_{\mathbf{K}}^2 = \mathbf{w}^\top \mathbf{K} \mathbf{w}$ is the norm with respect to the gram matrix.

– **Benchmark algorithms:** We compare RFN (as described in Algorithm 1) with three other benchmarks, listed below:

1. **Newton:** The exact Newton method $\mathbf{w}_{t+1} = \mathbf{w}_t + \alpha_t \mathbf{p}_t$, where \mathbf{p}_t is the exact solution of the linear system $\mathbf{H}(\mathbf{w}_t) \mathbf{p}_t = -\nabla F(\mathbf{w}_t)$.
2. **SSNCG:** The sub-sampled Newton method with conjugate gradient update $\mathbf{w}_{t+1} = \mathbf{w}_t + \alpha_t \mathbf{p}_t$, where \mathbf{p}_t is computed by solving the linear system $\widehat{\mathbf{H}}_{\text{SSN}}(\mathbf{w}_t) \mathbf{p}_t = -\nabla F(\mathbf{w}_t)$ up to a high precision by the CG method. The approximated Hessian $\widehat{\mathbf{H}}_{\text{SSN}}(\mathbf{w}_t)$ is generated as described in Section 2.4 (see (13)-(14)), i.e.,

$$\widehat{\mathbf{H}}_{\text{SSN}}(\mathbf{w}) = \sum_{i \in \mathcal{I}} [\mathbf{D}(\mathbf{w})]_{ii} \mathbf{K}(\mathcal{V}, i) \mathbf{K}(i, \mathcal{V}) + \lambda \mathbf{K}(\mathcal{V}, \mathcal{I}) \mathbf{K}(\mathcal{I}, \mathcal{I})^\dagger \mathbf{K}(\mathcal{I}, \mathcal{V}),$$

where \mathcal{I} is a random subset. We also add a regularization term $\mu \mathbf{I}$ to the above to avoid singularity.

3. **L-BFGS:** Limited-memory BFGS which approximates the Newton direction using the first order information. Here, we implement BFGS using the history of the past 50 updates of \mathbf{w}_t and $\nabla F(\mathbf{w}_t)$.

For all these methods, the step size α_t is determined by Armijo backtracking line search, and the full gradient $\nabla F(\mathbf{w}_t)$ is used. For SSNCG, the linear system is solved approximately to achieve 10^{-6} relative error.

– **Hyper-parameters of the empirical risk:** There are two hyper-parameters in the regularized kernel logistic regression: σ and λ . λ determines the rate by which we impose the RKHS norm as a penalty

Table 2: Descriptions of datasets used in the experiments.

Data set	Data points	Features	References
Covertypes	581012	54	[36]
Cod-RNA	59535	8	[37]

function. When λ is small, the model fits the training data. On the other hand, σ determines the kernel characteristics. As it grows larger, the gram matrix gets closer to a full-rank matrix, and this in turns increases the number of random features (or the number of sub-sampled data points) that randomized optimization methods (i.e., SSNCG and RFN) require to achieve good approximations of the original Hessian.

– **Hyper-parameter of backtracking line search:** We use a simple grid search to optimize the parameters for Newton and L-BFGS. However, due to the randomness of the approximated Hessian for randomized methods, we perform the line search adaptively for both SSNCG and RFN. For each iteration, the initial step size of backtracking is set as twice of the step size chosen in the previous iteration. This allows the algorithms to avoid staying in the search loop for long.

– **Datasets:** We apply all of the methods on two datasets from the UCI Machine Learning Repository (Table 2). For each dataset, we randomly select 5000 data points for training to run the optimization.

Covertypes: For this data set, the hyper-parameters of the objective function are set as follows: $\sigma = 0.5$, $\lambda = 10^{-5}$. For backtracking, we have two setups for randomized methods and non-randomized methods, respectively. For Newton and L-BFGS, $\alpha = 0.3$, $\beta = 0.5$ and the initial step size of backtracking is always set as 1. For SSNCG and RFN, $\alpha = 0.3$, $\beta = 0.2$ and the initial step size of backtracking is set as the inverse of squared Newton decrement.

Cod-RNA: For this data set, the hyper-parameters are set as follows: $\sigma = 2$; $\lambda = 10^{-5}$; $\alpha = 0.3$, $\beta = 0.5$ for Newton and L-BFGS and $\alpha = 0.3$, $\beta = 0.25$ for SSNCG and RFN.

For the number of random features for RFN (m) and the number of sub-sampled data points for SS-

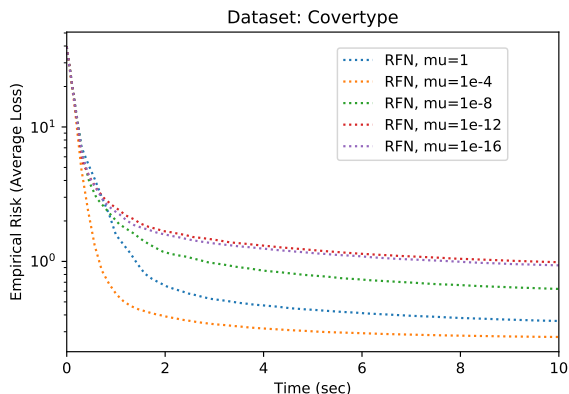


Figure 2: Sensitivity of empirical risk to μ .

NCG ($|Z|$), we set the ratio as 10% of the training data for both data sets. To prevent the approximated Hessians of RFN and SSNCG from being singular, a regularizer term $\mu\mathbf{I}$ is added with $\mu = 10^{-4}$.

– **Performance:** We record the loss value and the time cost of each iteration for all methods. The time cost includes the time of finding the Newton direction (computing the Hessian and solving the linear system) and determining the step size. The run time is obtained on a desktop with an 8-core, 3.00 Intel Core i7-9700 CPU and 15.5G of RAM (2666Mhz). The initial point \mathbf{w}_0 is generated from a standard Gaussian distribution. We run the experiment 40 times and calculate the standard errors for both loss value and time cost.

Based on Fig. 1, we see that the two randomized methods outperform the classical Newton method with time cost benefits from a small number of random features (or sub-sampled data points). RFN also outperforms L-BFGS, which approximates the newton direction using the first order information.

– **Sensitivity to μ :** To evaluate the sensitivity of RFN to the value of μ , we run the experiment of Covertypes data set with the same hyper parameter setting except μ . For this experiment, we choose $\mu \in \{1, 10^{-4}, 10^{-8}, 10^{-12}, 10^{-16}\}$. For each μ , we run the simulation 10 times and obtain the averaged

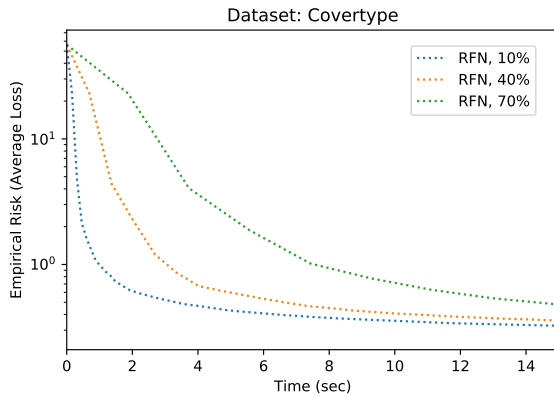


Figure 3: Empirical risk vs. time cost for different ratios of m/n .

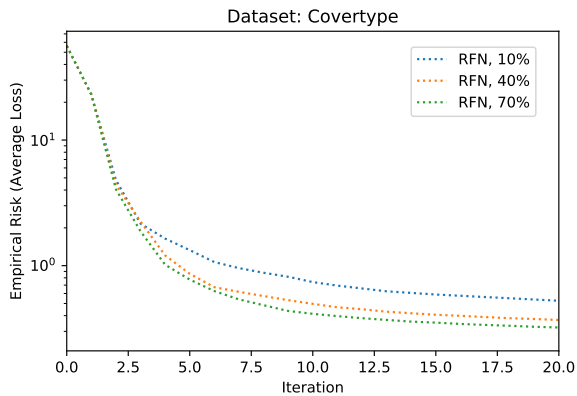


Figure 4: Empirical risk vs. iterations for different ratios of m/n .

loss. Based on Fig. 2, we find out that when μ is too small, the convergence rate is adversely affected by the singularity of the approximated Hessian. On the other hand, if the value of μ is too large, the regularizer dominates and RFN tends to behave like gradient descent. There is, however, a sweet spot in between where RFN performs best. Of course, this sweet spot entirely depends on the kernel choice and dataset, and it would be different across different problem environments.

– **Performance for various numbers of features m :** Another factor affecting the convergence performance of RFN is the number of random features. To see this property, we run the experiment on

Table 3: Performance comparison of Newton method, RFN, and dimension-reduced Newton method.

Model	Empirical Loss	Classification Rate (Training)	Classification Rate (Test)
Newton	0.31	100%	85.56%
RFN	0.31	100%	85.56%
Newton (dimension-reduced)	0.643	63.22%	49.82%

Covertypes data set with the same hyper-parameter set up except that μ is fixed as 10^{-6} and the ratio (m/n) ranges in the set 10%, 40%, 70%. Figs. 3- 4 verify that with more random features, the convergence is faster in terms of iterations, but this comes at the cost of increased run time. Using more random features improves the Hessian approximation, but it also increases the size of matrix \mathbf{C} in (12), which needs to be inverted.

– **Using random features as a dimension reduction technique:** For the optimization problem defined in RKHS as (2), one way to reduce the computation cost is to transform the original problem to another problem in a lower dimension [38] as

$$F(\mathbf{w}') = \sum_{i=1}^n \ell(y_i, [\mathbf{Z}\mathbf{w}']_i) + \frac{\lambda}{2} \mathbf{w}'^\top \mathbf{w}',$$

where \mathbf{Z} is defined in (8), $\mathbf{w}' = \mathbf{Z}^\top \mathbf{w} \in \mathbb{R}^m$, and $[\mathbf{x}]_i$ denotes the i -th element of \mathbf{x} . If Newton method is applied to this dimension-reduced problem directly, the computation cost per round is $O(m^3)$, which is less than $O(m^2n)$, the cost of each iteration for RFN (assuming that $m < n$). However, compared to RFN, this method finds the solution in a lower dimensional space instead of optimizing in the original functional space. It is interesting to see how this impacts the loss value and classification rate. We consider the same loss function defined in (28) where $\sigma = 10$ and $\lambda = 10^{-5}$. The ratio of random features (m/n) is set as 10% and $\mu = 10^{-4}$. We select 8000 data points (5000 for training and 3000 for testing) from Covertypes dataset and run the experiment for 10 times. The averaged empirical loss and averaged classification rates on the training and test datasets are tabulated in Table 3. We can see that, compared to RFN, applying Newton to random features has worse performance on both training and test

datasets. This is due to the fact that though approximating the update process, RFN still searches for the solution in the original functional space.

5 Conclusion

In this paper, we proposed a random-feature based Newton method (RFN) for risk minimization over RKHS. We drew explicit connections between the Hessian and the gram matrix and observed that sub-sampled Newton methods are not directly applicable to this optimization problem. Then, we showed that the Newton method can be expedited by applying kernel approximation techniques. From the theoretical point of view, we proved that the approximate Hessian is close to the original Hessian in terms of spectral norm when enough random features are sampled, which in turn ensures the local and global convergence with high probability. From the practical point of view, we applied RFN to two real-world data sets, compared it with three other benchmarks, and showed that RFN enjoys a faster run time under certain conditions. Future directions include the development of distributed/decentralized variants of RFN as well as data-dependent sampling schemes for random features [39].

6 Appendix

We make use of the matrix Bernstein inequality [29] for the proof of Lemma 2, but we adopt the version used in [34] and present it for real matrices.

Lemma 8. (*Matrix Concentration Inequality*) *Let \mathbf{B} be a fixed $d_1 \times d_2$ matrix. Consider a $d_1 \times d_2$ random matrix \mathbf{R} that satisfies*

$$\mathbb{E}[\mathbf{R}] = \mathbf{B} \quad \text{and} \quad \|\mathbf{R}\|_2 \leq U.$$

Let \mathbf{M}_1 and \mathbf{M}_2 be semi-definite upper bounds such that

$$\mathbb{E}[\mathbf{R}\mathbf{R}^\top] \preceq \mathbf{M}_1 \quad \text{and} \quad \mathbb{E}[\mathbf{R}^\top\mathbf{R}] \preceq \mathbf{M}_2.$$

Define the quantities

$$c \triangleq \max(\|\mathbf{M}_1\|_2, \|\mathbf{M}_2\|_2) \quad \text{and} \quad b \triangleq (\text{Tr}(\mathbf{M}_1) + \text{Tr}(\mathbf{M}_2))/c.$$

Form the matrix sampling estimator

$$\bar{\mathbf{R}}_h = \frac{1}{h} \sum_{i=1}^h \mathbf{R}_i,$$

where each \mathbf{R}_i is an independent copy of \mathbf{R} . Then, for all $\epsilon \geq \sqrt{c/h} + 2U/3h$,

$$\text{Pr}(\|\bar{\mathbf{R}}_h - \mathbf{B}\|_2 \geq \epsilon) \leq 4b \exp\left(\frac{-h\epsilon^2/2}{c + 2U\epsilon/3}\right).$$

6.1 Proof of Lemma 2

In the proof of this lemma, we disregard the dependence on \mathbf{w} and denote $\widehat{\mathbf{H}}(\mathbf{w})$, $\mathbf{H}(\mathbf{w})$ and $\mathbf{D}(\mathbf{w})$ by $\widehat{\mathbf{H}}$, \mathbf{H} and \mathbf{D} , respectively. The introduced shorthand is just for the sake of presentation clarity.

Our goal is to find the probability bound for the norm of the difference between the approximated Hessian $\widehat{\mathbf{H}}$ and the original Hessian \mathbf{H} :

$$\left\| \widehat{\mathbf{H}} - \mathbf{H} \right\| = \left\| (\mathbf{Z}\mathbf{Z}^\top \mathbf{D}\mathbf{Z}\mathbf{Z}^\top + \lambda\mathbf{Z}\mathbf{Z}^\top) - (\mathbf{K}\mathbf{D}\mathbf{K} + \lambda\mathbf{K}) \right\|.$$

Since $\|\mathbf{A} + \mathbf{B}\| \leq \|\mathbf{A}\| + \|\mathbf{B}\|$, we will find the bounds for $\|\mathbf{Z}\mathbf{Z}^\top \mathbf{D}\mathbf{Z}\mathbf{Z}^\top - \mathbf{K}\mathbf{D}\mathbf{K}\|$ and $\|\lambda\mathbf{Z}\mathbf{Z}^\top - \lambda\mathbf{K}\|$ in two parts, namely **Part 1** and **Part 2**, respectively.

Part 1:

First, we denote $\mathbf{z}(\omega_i)$ by \mathbf{z}_i . Then, $\mathbf{Z}\mathbf{Z}^\top \mathbf{D}\mathbf{Z}\mathbf{Z}^\top$ can be written as

$$\mathbf{Z}\mathbf{Z}^\top \mathbf{D}\mathbf{Z}\mathbf{Z}^\top = \frac{1}{m^2} \sum_{i=1}^m \sum_{j=1}^m \mathbf{z}_i \mathbf{z}_i^\top \mathbf{D} \mathbf{z}_j \mathbf{z}_j^\top.$$

For this summation, when $i \neq j$, we have that $\mathbb{E}[\mathbf{z}_i \mathbf{z}_i^\top \mathbf{D} \mathbf{z}_j \mathbf{z}_j^\top] = \mathbf{K}\mathbf{D}\mathbf{K}$. Based on this fact, we apply Lemma 8 as follows.

First, we know that

$$\left\| \mathbf{z}_i \mathbf{z}_i^\top \mathbf{D} \mathbf{z}_j \mathbf{z}_j^\top \right\| \leq \left\| \mathbf{z}_i \mathbf{z}_i^\top \right\| \|\mathbf{D}\| \left\| \mathbf{z}_j \mathbf{z}_j^\top \right\| \leq \lambda_1 n^2 \triangleq U.$$

as $\left\| \mathbf{z}_i \mathbf{z}_i^\top \right\| = \mathbf{z}_i^\top \mathbf{z}_i \leq n$ by the definition of \mathbf{z}_i in (7). On the other hand, since $\|\mathbf{D}(\mathbf{w})\| \leq \lambda_1$, we have that

$$\mathbf{z}_i^\top \mathbf{D} \mathbf{z}_j \leq \lambda_1 n,$$

and therefore,

$$\mathbf{z}_i \mathbf{z}_i^\top \mathbf{D} \mathbf{z}_j \mathbf{z}_j^\top \mathbf{z}_j \mathbf{z}_j^\top \mathbf{D} \mathbf{z}_i \mathbf{z}_i^\top \preceq \lambda_1^2 n^2 \text{Tr}(\mathbf{z}_j \mathbf{z}_j^\top) \mathbf{z}_i \mathbf{z}_i^\top.$$

Taking expectation from above, we derive

$$\mathbb{E}[\mathbf{z}_i \mathbf{z}_i^\top \mathbf{D} \mathbf{z}_j \mathbf{z}_j^\top \mathbf{z}_j \mathbf{z}_j^\top \mathbf{D} \mathbf{z}_i \mathbf{z}_i^\top] \preceq \lambda_1^2 n^2 \text{Tr}(\mathbf{K}) \mathbf{K} \triangleq \mathbf{M}_1.$$

By symmetry, we also have $\mathbf{M}_2 = \mathbf{M}_1$. Now, we can calculate quantities c and b in Lemma 8 as follows

$$\begin{aligned} c &= \lambda_1^2 n^2 \text{Tr}(\mathbf{K}) \|\mathbf{K}\| \\ b &= \frac{2\text{Tr}(\mathbf{M}_1)}{c} = \frac{2\text{Tr}(\mathbf{K})}{\|\mathbf{K}\|}. \end{aligned}$$

Noting that we have a total of $m^2 - m$ terms for which $i \neq j$, and using the above quantities, we get

$$\begin{aligned} & \Pr \left(\left\| \frac{1}{m^2 - m} \sum_{i \neq j} \mathbf{z}_i \mathbf{z}_i^\top \mathbf{D} \mathbf{z}_j \mathbf{z}_j^\top - \mathbf{K} \mathbf{D} \mathbf{K} \right\| \geq \epsilon \right) \\ & \leq 4b \exp \left(\frac{-(m^2 - m)\epsilon^2/2}{\lambda_1^2 n^2 \text{Tr}(\mathbf{K}) \|\mathbf{K}\| + \frac{2}{3} \lambda_1 n^2 \epsilon} \right). \end{aligned}$$

To have the right hand side smaller than δ , we should solve the inequality

$$\log \frac{4b}{\delta} \leq \frac{(m^2 - m)\epsilon^2/2}{\lambda_1^2 n^2 \text{Tr}(\mathbf{K}) \|\mathbf{K}\| + \frac{2}{3} \lambda_1 n^2 \epsilon}.$$

for m . Since $m \geq 2$, and thus $m^2 - m \geq \frac{1}{2}m^2$, it is sufficient to have

$$\frac{1}{4}m^2 \geq \frac{\lambda_1^2 n^2 \text{Tr}(\mathbf{K}) \|\mathbf{K}\| + \frac{2}{3} \lambda_1 n^2 \epsilon}{\epsilon^2} \log \frac{4b}{\delta}.$$

Therefore, with

$$m \geq \frac{2\sqrt{(\lambda_1^2 n^2 \text{Tr}(\mathbf{K}) \|\mathbf{K}\| + \frac{2}{3}\lambda_1 n^2 \epsilon) \log \frac{4b}{\delta}}}{\epsilon}, \quad (29)$$

we have with probability at least $1 - \delta$ that

$$\left\| \frac{1}{m^2 - m} \sum_{i \neq j} \mathbf{z}_i \mathbf{z}_i^\top \mathbf{D} \mathbf{z}_j \mathbf{z}_j^\top - \mathbf{K} \mathbf{D} \mathbf{K} \right\| < \epsilon.$$

Now, returning to $\|\mathbf{Z} \mathbf{Z}^\top \mathbf{D} \mathbf{Z} \mathbf{Z}^\top - \mathbf{K} \mathbf{D} \mathbf{K}\|$, we can re-write it as follows

$$\begin{aligned} & \left\| \frac{1}{m^2} \sum_{i \neq j} \mathbf{z}_i \mathbf{z}_i^\top \mathbf{D} \mathbf{z}_j \mathbf{z}_j^\top + \frac{1}{m^2} \sum_{i=j} \mathbf{z}_i \mathbf{z}_i^\top \mathbf{D} \mathbf{z}_j \mathbf{z}_j^\top - \mathbf{K} \mathbf{D} \mathbf{K} \right\| \\ & \leq \frac{m^2 - m}{m^2} \left\| \frac{1}{m^2 - m} \sum_{i \neq j} \mathbf{z}_i \mathbf{z}_i^\top \mathbf{D} \mathbf{z}_j \mathbf{z}_j^\top - \mathbf{K} \mathbf{D} \mathbf{K} \right\| \\ & \quad + \frac{1}{m^2} \left\| \sum_{i=j} \mathbf{z}_i \mathbf{z}_i^\top \mathbf{D} \mathbf{z}_j \mathbf{z}_j^\top \right\| + \frac{1}{m} \|\mathbf{K} \mathbf{D} \mathbf{K}\|. \end{aligned}$$

The first term is bounded by ϵ if (29) holds. For the second and third terms, we have

$$\frac{1}{m^2} \left\| \sum_{i=j} \mathbf{z}_i \mathbf{z}_i^\top \mathbf{D} \mathbf{z}_j \mathbf{z}_j^\top \right\| \leq \frac{1}{m^2} m \lambda_1 n^2 = \frac{1}{m} \lambda_1 n^2$$

and

$$\frac{1}{m} \|\mathbf{K} \mathbf{D} \mathbf{K}\| \leq \frac{1}{m} \lambda_1 n^2.$$

If $m \geq \frac{\lambda_1 n^2}{\epsilon}$, then the second and third terms are also bounded by ϵ . Combining these with (29), we require

$$m \geq \max \left\{ \frac{2\sqrt{(\lambda_1^2 n^2 \text{Tr}(\mathbf{K}) \|\mathbf{K}\| + \frac{2}{3}\lambda_1 n^2 \epsilon) \log \frac{4b}{\delta}}}{\epsilon}, \frac{\lambda_1 n^2}{\epsilon} \right\}$$

to guarantee that $\|\mathbf{Z} \mathbf{Z}^\top \mathbf{D} \mathbf{Z} \mathbf{Z}^\top - \mathbf{K} \mathbf{D} \mathbf{K}\|$ is bounded by 3ϵ with probability at least $(1 - \delta)$. Since we further assume that $\epsilon \leq \frac{3}{2}\lambda_1 \text{Tr}(\mathbf{K}) \|\mathbf{K}\|$, the sufficient lower bound on m can be simplified to

$$m \geq \max \left\{ \frac{4\sqrt{\frac{1}{3}\lambda_1^2 n^2 \text{Tr}(\mathbf{K}) \|\mathbf{K}\| \log \frac{4b}{\delta}}}{\epsilon}, \frac{\lambda_1 n^2}{\epsilon} \right\}.$$

Since both $\text{Tr}(\mathbf{K})$ and $\|\mathbf{K}\|$ are bounded above by n , the above inequality implies that a sufficient condition for m is below

$$m = \Omega\left(\frac{\lambda_1 n^2}{\epsilon} \sqrt{\log \frac{n}{\delta}}\right). \quad (30)$$

Part 2:

Now, we turn to $\|\lambda \mathbf{Z} \mathbf{Z}^\top - \lambda \mathbf{K}\|$, which can be written as $\|\frac{\lambda}{m} \sum_{i=1}^m \mathbf{z}_i \mathbf{z}_i^\top - \lambda \mathbf{K}\|$. Notice that $\mathbb{E}[\mathbf{z}_i \mathbf{z}_i^\top] = \mathbf{K}$. To apply Lemma 8, we observe that

$$\|\lambda \mathbf{z}_i \mathbf{z}_i^\top\| \leq \lambda n \triangleq U,$$

and

$$\mathbb{E}[\lambda^2 \mathbf{z}_i \mathbf{z}_i^\top \mathbf{z}_i \mathbf{z}_i^\top] \preceq \lambda^2 n \mathbf{K} \triangleq \mathbf{M}_1.$$

Again, by symmetry $\mathbf{M}_1 = \mathbf{M}_2$, and also we have that

$$c = \lambda^2 n \|\mathbf{K}\|$$

$$b = \frac{2\text{Tr}(\mathbf{M}_1)}{c} = \frac{2\text{Tr}(\mathbf{K})}{\|\mathbf{K}\|}.$$

With the above quantities, based on Lemma 8, we derive

$$\Pr\left(\left\|\frac{\lambda}{m} \sum_i \mathbf{z}_i \mathbf{z}_i^\top - \lambda \mathbf{K}\right\| \geq \epsilon\right)$$

$$\leq 4b \exp \frac{-m\epsilon^2/2}{\lambda^2 n \|\mathbf{K}\| + \frac{2}{3} \lambda n \epsilon}.$$

To have the right hand side smaller than δ , we should solve the inequality

$$\log \frac{4b}{\delta} \leq \frac{m\epsilon^2/2}{\lambda^2 n \|\mathbf{K}\| + \frac{2}{3} \lambda n \epsilon},$$

for m , which implies

$$m \geq \frac{2\lambda^2 n \|\mathbf{K}\| + \frac{4}{3} \lambda n \epsilon}{\epsilon^2} \log \frac{4b}{\delta}.$$

Since we further assume that $\epsilon \leq \frac{3}{2}\lambda \|\mathbf{K}\|$, the sufficient lower bound on m can be simplified to

$$m \geq \frac{\frac{8}{3}\lambda^2 n \|\mathbf{K}\|}{\epsilon^2} \log \frac{4b}{\delta}.$$

As both $\text{Tr}(\mathbf{K})$ and $\|\mathbf{K}\|$ are bounded above by n , the sufficient condition for m becomes

$$m = \Omega \left(\frac{\lambda^2 n^2}{\epsilon^2} \log \frac{n}{\delta} \right). \quad (31)$$

Now, by combining (30) and (31), we have that if

$$m = \Omega \left(\frac{n^2}{\epsilon} \max \left\{ \frac{\lambda^2}{\epsilon} \log \frac{n}{\delta}, \lambda_1 \sqrt{\log \frac{n}{\delta}} \right\} \right),$$

then $\|\widehat{\mathbf{H}} - \mathbf{H}\|$ is bounded by 4ϵ with probability at least $(1 - \delta)$.

Our convergence results are in high probability, similar to those presented in [4]. The main difference is in the Hessian approximation technique, which in our case is specific to risk minimization in RKHS.

6.2 Proof of Theorem 4

Denote the minimum eigenvalue of $\widehat{\mathbf{H}}_\mu(\mathbf{w}_t)$ by $\lambda_{\min}(\widehat{\mathbf{H}}_\mu(\mathbf{w}_t))$, and recall that $\mathbf{p}_t \triangleq -[\widehat{\mathbf{H}}_\mu(\mathbf{w}_t)]^{-1} \nabla F(\mathbf{w}_t)$.

Since

$$\mathbf{p}_t^\top \widehat{\mathbf{H}}_\mu(\mathbf{w}_t) \mathbf{p}_t \geq \lambda_{\min}(\widehat{\mathbf{H}}_\mu(\mathbf{w}_t)) \|\mathbf{p}_t\|^2,$$

by Corollary 3 (Equation (19)), we have that

$$\mathbf{p}_t^\top \widehat{\mathbf{H}}_\mu(\mathbf{w}_t) \mathbf{p}_t \geq [(1 - \Psi)\gamma + \mu] \|\mathbf{p}_t\|^2.$$

For any $\alpha > 0$, define $\mathbf{w}_\alpha \triangleq \mathbf{w}_t + \alpha \mathbf{p}_t$. With L -smoothness of the objective function F , we have

$$\begin{aligned} & F(\mathbf{w}_\alpha) - F(\mathbf{w}_t) \\ & \leq (\mathbf{w}_\alpha - \mathbf{w}_t)^\top \nabla F(\mathbf{w}_t) + \frac{L}{2} \|\mathbf{w}_\alpha - \mathbf{w}_t\|^2 \\ & = \alpha \mathbf{p}_t^\top \nabla F(\mathbf{w}_t) + \frac{\alpha^2 L}{2} \|\mathbf{p}_t\|^2. \end{aligned}$$

To pass the Amijo line-search, we need an α which makes the following inequality hold

$$\alpha \mathbf{p}_t^\top \nabla F(\mathbf{w}_t) + \frac{\alpha^2 L}{2} \|\mathbf{p}_t\|^2 \leq \alpha \beta \mathbf{p}_t^\top \nabla F(\mathbf{w}_t).$$

Since $\mathbf{p}_t^\top \nabla F(\mathbf{w}_t) = -\mathbf{p}_t^\top \widehat{\mathbf{H}}_\mu(\mathbf{w}_t) \mathbf{p}_t$, the above inequality can be written as

$$\alpha L \|\mathbf{p}_t\|^2 \leq 2(1 - \beta) \mathbf{p}_t^\top \widehat{\mathbf{H}}_\mu(\mathbf{w}_t) \mathbf{p}_t.$$

Therefore, if

$$\alpha \leq 2(1 - \beta)[(1 - \Psi)\gamma + \mu]/L,$$

(given that $\mathbf{p}_t^\top \widehat{\mathbf{H}}_\mu(\mathbf{w}_t) \mathbf{p}_t \geq [(1 - \Psi)\gamma + \mu] \|\mathbf{p}_t\|^2$), the Armijo line search is satisfied. This quantity is iteration-independent. Now, $\mathbf{w}_{t+1} = \mathbf{w}_t + \alpha_t^\top \mathbf{p}_t$, and based on (22), we have that

$$\begin{aligned} F(\mathbf{w}_{t+1}) &\leq F(\mathbf{w}_t) + \alpha_t \beta \mathbf{p}_t^\top \nabla F(\mathbf{w}_t) \\ &= F(\mathbf{w}_t) - \alpha_t \beta \nabla F(\mathbf{w}_t)^\top [\widehat{\mathbf{H}}_\mu(\mathbf{w}_t)]^{-1} \nabla F(\mathbf{w}_t) \\ &\leq F(\mathbf{w}_t) - \alpha_t \beta \frac{\|\nabla F(\mathbf{w}_t)\|^2}{[(1 + \Psi)L + \mu]}, \end{aligned}$$

where the last inequality comes from (19). By subtracting $F(\mathbf{w}^*)$ from both sides and noting that $F(\mathbf{w}_t) - F(\mathbf{w}^*) \leq \frac{\|\nabla F(\mathbf{w}_t)\|^2}{2\gamma}$ due to the strong convexity of F , the result is proved.

Lemma 9. (*Error recursion*) *Let Assumption 2 hold. Assume that $\alpha_t = 1$ and $\widehat{\mathbf{H}}_\mu(\mathbf{w})$ is positive definite.*

We then have

$$\|\mathbf{w}_{t+1} - \mathbf{w}^*\| \leq \nu \|\mathbf{w}_t - \mathbf{w}^*\| + \eta \|\mathbf{w}_t - \mathbf{w}^*\|^2,$$

where $\eta \triangleq \frac{M}{2\lambda_{\min}(\widehat{\mathbf{H}}_\mu(\mathbf{w}_t))}$ and $\nu \triangleq \frac{\|\widehat{\mathbf{H}}_\mu(\mathbf{w}_t) - \mathbf{H}(\mathbf{w}_t)\|}{\lambda_{\min}(\widehat{\mathbf{H}}_\mu(\mathbf{w}_t))}$.

6.3 Proof of Lemma 9

Define $\Delta_t \triangleq \mathbf{w}_t - \mathbf{w}^*$. Since

$$\mathbf{w}_{t+1} = \mathbf{w}_t - \widehat{\mathbf{H}}_\mu(\mathbf{w}_t)^{-1} \nabla F(\mathbf{w}_t),$$

\mathbf{w}_{t+1} is the optimal solution of the following second order approximation:

$$\begin{aligned} N(\mathbf{w}) &= F(\mathbf{w}_t) + (\mathbf{w} - \mathbf{w}_t)^\top \nabla F(\mathbf{w}_t) \\ &\quad + \frac{1}{2} (\mathbf{w} - \mathbf{w}_t)^\top \widehat{\mathbf{H}}_\mu(\mathbf{w}_t) (\mathbf{w} - \mathbf{w}_t). \end{aligned}$$

Based on that, for any $\mathbf{w} \in \mathbb{R}^n$, we have

$$\begin{aligned} 0 &= (\mathbf{w} - \mathbf{w}_{t+1})^\top \nabla N(\mathbf{w}_{t+1}) \\ &= (\mathbf{w} - \mathbf{w}_{t+1})^\top \nabla F(\mathbf{w}_t) + (\mathbf{w} - \mathbf{w}_{t+1})^\top \widehat{\mathbf{H}}_\mu(\mathbf{w}_t)(\mathbf{w}_{t+1} - \mathbf{w}_t). \end{aligned}$$

By setting $\mathbf{w} = \mathbf{w}^*$ and noting that $\mathbf{w}_{t+1} - \mathbf{w}_t = \Delta_{t+1} - \Delta_t$, we have

$$\begin{aligned} \Delta_{t+1}^\top \widehat{\mathbf{H}}_\mu(\mathbf{w}_t) \Delta_{t+1} &= \Delta_{t+1}^\top \widehat{\mathbf{H}}_\mu(\mathbf{w}_t) \Delta_t - \Delta_{t+1}^\top \nabla F(\mathbf{w}_t) \\ &\quad + \Delta_{t+1}^\top \nabla F(\mathbf{w}^*), \end{aligned}$$

as $\nabla F(\mathbf{w}^*) = 0$ due to the optimality of \mathbf{w}^* . By the mean value theorem, we have

$$\begin{aligned} &\nabla F(\mathbf{w}_t) - \nabla F(\mathbf{w}^*) \\ &= \left(\int_0^1 \nabla^2 F(\mathbf{w}^* + \tau(\mathbf{w}_t - \mathbf{w}^*)) d\tau \right) (\mathbf{w}_t - \mathbf{w}^*). \end{aligned}$$

Therefore,

$$\begin{aligned} &\Delta_{t+1}^\top \widehat{\mathbf{H}}_\mu(\mathbf{w}_t) \Delta_{t+1} \\ &= \Delta_{t+1}^\top \widehat{\mathbf{H}}_\mu(\mathbf{w}_t) \Delta_t - \Delta_{t+1}^\top \left(\int_0^1 \nabla^2 F(\mathbf{w}^* + \tau(\mathbf{w}_t - \mathbf{w}^*)) d\tau \right) \Delta_t \\ &= \Delta_{t+1}^\top \widehat{\mathbf{H}}_\mu(\mathbf{w}_t) \Delta_t - \Delta_{t+1}^\top \nabla^2 F(\mathbf{w}_t) \Delta_t \\ &\quad + \Delta_{t+1}^\top \nabla^2 F(\mathbf{w}_t) \Delta_t - \Delta_{t+1}^\top \left(\int_0^1 \nabla^2 F(\mathbf{w}^* + \tau(\mathbf{w}_t - \mathbf{w}^*)) d\tau \right) \Delta_t \\ &\leq \|\Delta_{t+1}\| \left\| \widehat{\mathbf{H}}_\mu(\mathbf{w}_t) - \nabla^2 F(\mathbf{w}_t) \right\| \|\Delta_t\| \\ &\quad + \|\Delta_{t+1}\| \left(\int_0^1 \left\| \nabla^2 F(\mathbf{w}_t) - \nabla^2 F(\mathbf{w}^* + \tau(\mathbf{w}_t - \mathbf{w}^*)) \right\| d\tau \right) \|\Delta_t\| \\ &\leq \left\| \widehat{\mathbf{H}}_\mu(\mathbf{w}_t) - \nabla^2 F(\mathbf{w}_t) \right\| \|\Delta_t\| \|\Delta_{t+1}\| + \frac{M}{2} \|\Delta_t\|^2 \|\Delta_{t+1}\|. \end{aligned}$$

Since $\Delta_{t+1}^\top \widehat{\mathbf{H}}_\mu(\mathbf{w}_t) \Delta_{t+1} \geq \lambda_{\min}(\widehat{\mathbf{H}}_\mu(\mathbf{w}_t)) \|\Delta_{t+1}\|^2$ and $\widehat{\mathbf{H}}_\mu(\mathbf{w}_t)$ is assumed to be positive definite, the result follows.

6.4 Proof of Lemma 5

In view of Lemma 2 and Corollary 3, we know that $\left\| \widehat{\mathbf{H}}_{\mu}(\mathbf{w}_t) - \nabla^2 F(\mathbf{w}_t) \right\| \leq \Psi\gamma + \mu$ and $\lambda_{\min}(\widehat{\mathbf{H}}_{\mu}(\mathbf{w}_t)) \geq [(1 - \Psi)\gamma + \mu]$. The result follows by applying these to Lemma 9.

6.5 Proof of Theorem 6

By choosing ϵ based on this requirement, according to Lemma 5, we have $\|\mathbf{w}_{t+1} - \mathbf{w}^*\| \leq \nu \|\mathbf{w}_t - \mathbf{w}^*\| + \eta \|\mathbf{w}_t - \mathbf{w}^*\|^2$ for every t . The choice of \mathbf{w}_0 guarantees that

$$\nu \|\mathbf{w}_0 - \mathbf{w}^*\| + \eta \|\mathbf{w}_0 - \mathbf{w}^*\|^2 \leq \rho \|\mathbf{w}_0 - \mathbf{w}^*\|,$$

and the proof follows by induction.

The probability that all iterations are successful is the complement of the probability that at least one iteration fails, which is bounded by $t_0\delta$ (Boole's inequality). Therefore, the probability of a successful process is at least $(1 - t_0\delta)$.

References and Notes

- [1] L. Bottou, F. E. Curtis, and J. Nocedal, "Optimization methods for large-scale machine learning," *Siam Review*, vol. 60, no. 2, pp. 223–311, 2018.
- [2] Y. Nesterov, "Introductory lectures on convex programming volume i: Basic course," *Lecture notes*, vol. 3, no. 4, p. 5, 1998.
- [3] R. Bollapragada, R. H. Byrd, and J. Nocedal, "Exact and inexact subsampled newton methods for optimization," *IMA Journal of Numerical Analysis*, vol. 39, no. 2, pp. 545–578, 2018.
- [4] F. Roosta-Khorasani and M. W. Mahoney, "Sub-sampled newton methods," *Mathematical Programming*, vol. 174, no. 1-2, pp. 293–326, 2019.

- [5] P. Xu, J. Yang, F. Roosta-Khorasani, C. Ré, and M. W. Mahoney, “Sub-sampled newton methods with non-uniform sampling,” in *Advances in Neural Information Processing Systems*, 2016, pp. 3000–3008.
- [6] M. Pilanci and M. J. Wainwright, “Newton sketch: A near linear-time optimization algorithm with linear-quadratic convergence,” *SIAM Journal on Optimization*, vol. 27, no. 1, pp. 205–245, 2017.
- [7] C. G. Broyden, “The convergence of a class of double-rank minimization algorithms: 2. the new algorithm,” *IMA journal of applied mathematics*, vol. 6, no. 3, pp. 222–231, 1970.
- [8] R. Fletcher, “A new approach to variable metric algorithms,” *The computer journal*, vol. 13, no. 3, pp. 317–322, 1970.
- [9] D. Goldfarb, “A family of variable-metric methods derived by variational means,” *Mathematics of computation*, vol. 24, no. 109, pp. 23–26, 1970.
- [10] D. F. Shanno, “Conditioning of quasi-newton methods for function minimization,” *Mathematics of computation*, vol. 24, no. 111, pp. 647–656, 1970.
- [11] N. N. Schraudolph, J. Yu, and S. Günter, “A stochastic quasi-newton method for online convex optimization,” in *Artificial intelligence and statistics*, 2007, pp. 436–443.
- [12] A. Mokhtari and A. Ribeiro, “Res: Regularized stochastic bfgs algorithm,” *IEEE Transactions on Signal Processing*, vol. 62, no. 23, pp. 6089–6104, 2014.
- [13] R. H. Byrd, S. L. Hansen, J. Nocedal, and Y. Singer, “A stochastic quasi-newton method for large-scale optimization,” *SIAM Journal on Optimization*, vol. 26, no. 2, pp. 1008–1031, 2016.
- [14] P. Moritz, R. Nishihara, and M. Jordan, “A linearly-convergent stochastic l-bfgs algorithm,” in *Artificial Intelligence and Statistics*, 2016, pp. 249–258.

- [15] A. Bordes, L. Bottou, and P. Gallinari, “Sgd-qn: Careful quasi-newton stochastic gradient descent,” *Journal of Machine Learning Research*, vol. 10, no. Jul, pp. 1737–1754, 2009.
- [16] J. Sohl-Dickstein, B. Poole, and S. Ganguli, “Fast large-scale optimization by unifying stochastic gradient and quasi-newton methods,” in *International Conference on Machine Learning*, 2014, pp. 604–612.
- [17] A. Mokhtari and A. Ribeiro, “Global convergence of online limited memory bfgs,” *The Journal of Machine Learning Research*, vol. 16, no. 1, pp. 3151–3181, 2015.
- [18] A. Mokhtari, M. Eisen, and A. Ribeiro, “Iqn: An incremental quasi-newton method with local superlinear convergence rate,” *SIAM Journal on Optimization*, vol. 28, no. 2, pp. 1670–1698, 2018.
- [19] R. Gower, D. Goldfarb, and P. Richtárik, “Stochastic block bfgs: Squeezing more curvature out of data,” in *International Conference on Machine Learning*, 2016, pp. 1869–1878.
- [20] R. Zhao, W. B. Haskell, and V. Y. Tan, “Stochastic l-bfgs: Improved convergence rates and practical acceleration strategies,” *IEEE Transactions on Signal Processing*, vol. 66, no. 5, pp. 1155–1169, 2018.
- [21] J. Shawe-Taylor, N. Cristianini *et al.*, *Kernel methods for pattern analysis*. Cambridge university press, 2004.
- [22] A. Rahimi and B. Recht, “Random features for large-scale kernel machines,” in *Advances in neural information processing systems*, 2008, pp. 1177–1184.
- [23] R. H. Byrd, G. M. Chin, W. Neveitt, and J. Nocedal, “On the use of stochastic hessian information in optimization methods for machine learning,” *SIAM Journal on Optimization*, vol. 21, no. 3, pp. 977–995, 2011.

- [24] R. H. Byrd, G. M. Chin, J. Nocedal, and Y. Wu, “Sample size selection in optimization methods for machine learning,” *Mathematical programming*, vol. 134, no. 1, pp. 127–155, 2012.
- [25] C.-C. Wang, C.-H. Huang, and C.-J. Lin, “Subsampled hessian newton methods for supervised learning,” *Neural computation*, vol. 27, no. 8, pp. 1766–1795, 2015.
- [26] J. Martens, “Deep learning via hessian-free optimization.” in *ICML*, vol. 27, 2010, pp. 735–742.
- [27] M. A. Erdogdu and A. Montanari, “Convergence rates of sub-sampled newton methods,” in *NIPS*, 2015.
- [28] J. A. Tropp and S. J. Wright, “Computational methods for sparse solution of linear inverse problems,” *Proceedings of the IEEE*, vol. 98, no. 6, pp. 948–958, 2010.
- [29] J. A. Tropp *et al.*, “An introduction to matrix concentration inequalities,” *Foundations and Trends® in Machine Learning*, vol. 8, no. 1-2, pp. 1–230, 2015.
- [30] N. Agarwal, B. Bullins, and E. Hazan, “Second-order stochastic optimization for machine learning in linear time,” *The Journal of Machine Learning Research*, vol. 18, no. 1, pp. 4148–4187, 2017.
- [31] M. Mutny, “Stochastic second-order optimization via von neumann series,” *arXiv preprint arXiv:1612.04694*, 2016.
- [32] P. Kar and H. Karnick, “Random feature maps for dot product kernels,” in *International conference on Artificial Intelligence and Statistics*, 2012, pp. 583–591.
- [33] J. Yang, V. Sindhwani, Q. Fan, H. Avron, and M. W. Mahoney, “Random laplace feature maps for semigroup kernels on histograms,” in *Proceedings of the IEEE Conference on Computer Vision and Pattern Recognition*, 2014, pp. 971–978.

- [34] H. Avron, M. Kapralov, C. Musco, C. Musco, A. Velingker, and A. Zandieh, “Random fourier features for kernel ridge regression: Approximation bounds and statistical guarantees,” in *Proceedings of the 34th International Conference on Machine Learning-Volume 70*, 2017, pp. 253–262.
- [35] A. Gittens and M. W. Mahoney, “Revisiting the nyström method for improved large-scale machine learning,” *The Journal of Machine Learning Research*, vol. 17, no. 1, pp. 3977–4041, 2016.
- [36] J. A. Blackard and D. J. Dean, “Comparative accuracies of artificial neural networks and discriminant analysis in predicting forest cover types from cartographic variables,” *Computers and electronics in agriculture*, vol. 24, no. 3, pp. 131–151, 1999.
- [37] A. V. Uzilov, J. M. Keegan, and D. H. Mathews, “Detection of non-coding rnas on the basis of predicted secondary structure formation free energy change,” *BMC bioinformatics*, vol. 7, no. 1, p. 173, 2006.
- [38] A. Rahimi and B. Recht, “Weighted sums of random kitchen sinks: Replacing minimization with randomization in learning,” in *Advances in Neural Information Processing Systems*, 2009, pp. 1313–1320.
- [39] S. Shahrampour, A. Beirami, and V. Tarokh, “On data-dependent random features for improved generalization in supervised learning,” in *Thirty-Second AAAI Conference on Artificial Intelligence*, 2018.